Quantum Phase Transitions

SUBIR SACHDEV
Professor of Physics
Yale University

CAMBRIDGE
UNIVERSITY PRESS

PUBLISHED BY THE PRESS SYNDICATE OF THE UNIVERSITY OF CAMBRIDGE
The Pitt Building, Trumpington Street, Cambridge, United Kingdom

CAMBRIDGE UNIVERSITY PRESS
The Edinburgh Building, Cambridge CB2 2RU, UK http://www.cup.cam.ac.uk
40 West 20th Street, New York, NY 10011-4211, USA http: //www.cup.org
10 Stamford Road, Oakleigh, Melbourne 3166, Australia
Ruiz de Alarcón 13, 28014 Madrid, Spain

First published 1999

Printed in the United States of America

Typeface in Times Roman 10/12.5 pt. *System* LaTeX 2_ε [TB]

A catalog record for this book is available from
the British Library.

Library of Congress Cataloging-in-Publication Data
Sachdev, Subir, 1961–
Quantum phase transitions / Subir Sachdev.
p. cm.
Includes bibliographical references and index.
ISBN 0-521-58254-7
1. Phase transformations (Statistical physics) 2. Quantum theory.
I. Title.
QC175. 16.P5S23 2000
530.4′14 – dc21 99-12280
CIP

ISBN 0 521 58254 7 hardback

Contents

1

Basic Concepts

1.1 What Is a Quantum Phase Transition?

Consider a Hamiltonian, $H(g)$, whose degrees of freedom reside on the sites of a lattice, and which varies as a function of a dimensionless coupling g. Let us follow the evolution of the ground state energy of $H(g)$ as a function of g. For the case of a finite lattice, this ground state energy will generically be a smooth, analytic function of g. The main possibility of an exception comes from the case when g couples only to a conserved quantity (i.e., $H(g) = H_0 + gH_1$, where H_0 and H_1 commute). This means that H_0 and H_1 can be simultaneously diagonalized and so the eigenfunctions are independent of g even though the eigenvalues vary with g; then there can be a level-crossing where an excited level becomes the ground state at $g = g_c$ (say), creating a point of nonanalyticity of the ground state energy as a function of g (see Fig. 1.1). The possibilities for an *infinite* lattice are richer. An avoided level-crossing between the ground and an excited state in a finite lattice could become progressively sharper as the lattice size increases, leading to a nonanalyticity at $g = g_c$ in the infinite lattice limit. We shall identify any point of nonanalyticity in the ground state energy of the infinite lattice system as a quantum phase transition: The nonanalyticity could be either the limiting case of an avoided level-crossing or an actual level-crossing. The first kind is more common, but we shall also discuss transitions of the second kind in Chapters 11 and 13. The phase transition is usually accompanied by a qualitative change in the nature of the correlations in the ground state, and describing this change shall clearly be one of our major interests.

Actually our focus shall be on a limited class of quantum phase transitions – those that are *second order*. Loosely speaking, these are transitions at which the characteristic energy scale of fluctuations above the ground state vanishes as g approaches g_c. Let the energy Δ represent a scale characterizing some significant spectral density of fluctuations at zero temperature (T) for $g \neq g_c$. Thus Δ could be the energy of the lowest excitation above the ground state, if this is nonzero (i.e., there is an energy gap Δ), or if there are excitations at arbitrarily low energies in the infinite lattice limit (i.e., the energy spectrum is *gapless*), Δ is the scale at which there is a qualitative change in the nature of the frequency spectrum from its lowest frequency to its higher frequency behavior. In most cases, we will find that as g approaches g_c, Δ vanishes as

$$\Delta \sim J|g - g_c|^{z\nu} \tag{1.1}$$

(exceptions to this behavior appear in Section 14.2.6). Here J is the energy scale of a characteristic microscopic coupling, and $z\nu$ is a *critical exponent*. The value of $z\nu$ is usually

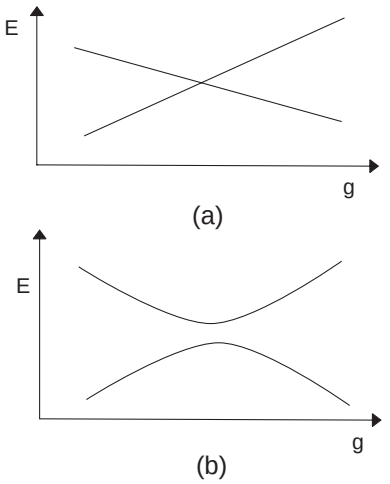

Figure 1.1. Low eigenvalues, E, of a Hamiltonian $H(g)$ on a finite lattice, as a function of some dimensionless coupling g. For the case where $H(g) = H_0 + gH_1$, where H_0 and H_1 commute and are independent of g, there can be an actual level-crossing, as in (a). More generally, however, there is an "avoided level-crossing," as in (b).

universal, that is, it is independent of most of the microscopic details of the Hamiltonian $H(g)$ (we shall have much more to say about the concept of universality below, and in the following chapters). The behavior (1.1) holds both for $g > g_c$ and for $g < g_c$ with the same value of the exponent $z\nu$, but with different nonuniversal constants of proportionality. We shall sometimes use the symbol Δ_+ (Δ_-) to represent the characteristic energy scale for $g > g_c$ ($g < g_c$).

In addition to a vanishing energy scale, second-order quantum phase transitions invariably have a diverging characteristic length scale ξ: This could be the length scale determining the exponential decay of equal-time correlations in the ground state or the length scale at which some characteristic crossover occurs to the correlations at the longest distances. This length diverges as

$$\xi^{-1} \sim \Lambda |g - g_c|^{\nu}, \tag{1.2}$$

where ν is a critical exponent, and Λ is an inverse length scale (a "momentum cutoff") of order the inverse lattice spacing. The ratio of the exponents in (1.1) and (1.2) is z, the dynamic critical exponent: The characteristic energy scale vanishes as the zth power of the characteristic inverse length scale

$$\Delta \sim \xi^{-z}. \tag{1.3}$$

It is important to notice that the discussion above refers to singularities in the *ground state* of the system. So strictly speaking, quantum phase transitions occur only at zero temperature, $T = 0$. Because all experiments are necessarily at some nonzero, though possibly very small, temperature, a central task of the theory of quantum phase transitions is to describe the consequences of this $T = 0$ singularity on physical properties at $T > 0$. It turns out that working outward from the quantum critical point at $g = g_c$ and $T = 0$ is a powerful way of understanding and describing the thermodynamic and dynamic properties of numerous systems over a broad range of values of $|g - g_c|$ and T. Indeed, it is not even

necessary that the system of interest ever have its microscopic couplings reach a value such that $g = g_c$: It can still be very useful to argue that there is a quantum critical point at a physically inaccessible coupling $g = g_c$ and to develop a description in the deviation $|g - g_c|$. It is one of the purposes of this book to describe the physical perspective that such an approach offers and to contrast it from more conventional expansions about very weak (say $g \to 0$) or very strong couplings (say $g \to \infty$).

1.2 Quantum Versus Classical Phase Transitions

There are two important possibilities for the $T > 0$ phase diagram of a system near a quantum critical point. These are shown in Fig. 1.2, and we will meet examples of both kinds in this book. In the first, shown in Fig. 1.2a, the thermodynamic singularity is present only at $T = 0$, and all $T > 0$ properties are analytic as a function of g near $g = g_c$. In the second, shown in Fig. 1.2b, there is a line of $T > 0$ second-order phase transitions (this is a line at which the thermodynamic free energy is not analytic) that terminates at the $T = 0$ quantum critical point at $g = g_c$. In the vicinity of such a line, we will find that the typical frequency at which the important long distance degrees of freedom fluctuate, $\omega_{\rm typ}$, satisfies

$$\hbar\omega_{\rm typ} \ll k_B T. \tag{1.4}$$

Under these conditions, it will be seen that a purely *classical* description can be applied to these important degrees of freedom – this classical description works in the shaded region of Fig. 1.2b. Consequently, the ultimate critical singularity along the line of $T > 0$ phase transitions in Fig. 1.2b is described by the theory of second-order phase transitions in classical systems. This theory was developed thoroughly in the past three decades and

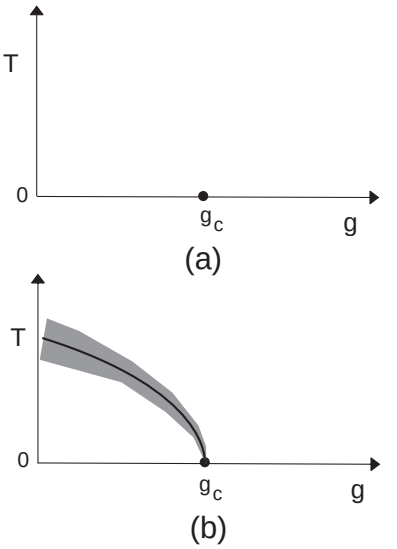

Figure 1.2. Two possible phase diagrams of system near a quantum phase transition. In both cases there is a quantum critical point at $g = g_c$ and $T = 0$. In (b), there is a line of $T > 0$ second-order phase transitions terminating at the quantum critical point. The theory of phase transitions in classical systems driven by thermal fluctuations can be applied with the shaded region of (b).

has been explained in many popular reviews and books [342, 65, 268, 196, 588]. We shall assume here that the reader has some familiarity with at least the basic concepts of this classical theory and will occasionally refer to some of these sources for specific details. Notice that the shaded region of classical behavior in Fig. 1.2b lies within the wider window of the phase diagram, with moderate values of $|g - g_c|$ and T, which we asserted above should be described as an expansion about the quantum critical point at $g = g_c$ and $T = 0$. So our study of quantum phase transitions will also apply to the shaded region of Fig. 1.2b, where it will yield information complementary to that available by directly thinking of the $T > 0$ phase transition in terms of purely classical models.

We note that phase transitions in classical models are driven only by thermal fluctuations, as classical systems usually freeze into a fluctuationless ground state at $T = 0$. In contrast, quantum systems have fluctuations driven by the Heisenberg uncertainty principle even in the ground state, and these can drive interesting phase transitions at $T = 0$. The $T > 0$ region in the vicinity of a quantum critical point therefore offers a fascinating interplay of effects driven by quantum and thermal fluctuations; sometimes, as in the shaded region of Fig. 1.2b, we can find some dominant, effective degrees of freedom whose fluctuations are purely classical and thermal, and then the classical theory will apply. However, as already noted, our attention will not be limited to such regions, and we shall be interested in a broader section of the phase diagram.

1.3 Experimental Examples

To make the concepts of the previous sections less abstract, let us mention some recent experimental studies of second-order quantum phase transitions. All of the following examples will also be discussed further in this book.

- The low-lying magnetic excitations of the insulator $LiHoF_4$ consist of fluctuations of the Ho ions between two spin states that are aligned parallel and antiparallel to a particular crystalline axis. These states can be represented by a two-state "Ising" spin variable on each Ho ion. At $T = 0$, the magnetic dipolar interactions between the Ho ions cause all the Ising spins to align in the same orientation, and so the ground state is a ferromagnet. Bitko, Rosenbaum, and Aeppli [56] placed this material in a magnetic field transverse to the magnetic axis. Such a field induces quantum tunneling between the two states of each Ho ion, and a sufficiently strong tunneling rate can eventually destroy the long-range magnetic order. Such a quantum phase transition was indeed observed [56], with the ferromagnetic moment vanishing continuously at a quantum critical point. Note that such a transition can, in principle, occur precisely at $T = 0$, when it is driven entirely by quantum fluctuations. We shall call the $T = 0$ state without magnetic order a *quantum paramagnet*. However, we can also destroy the magnetic order at a fixed transverse magnetic field (possibly zero), simply by raising the temperature, enabling the material to undergo a conventional Curie transition to a high-temperature magnetically disordered state. Among the objectives of this book is to provide a description of the intricate crossover between the zero-temperature quantum transition and the finite temperature transition driven partially by thermal fluctuations; we shall also delineate the important differences between the $T = 0$ quantum paramagnet and the high-temperature "thermal paramagnet;" see Chapters 5, 7, and 8.

- The heavy fermion material $CeCu_{6-x}Au_x$ [439, 514, 555, 477] has a magnetically ordered ground state, with the magnetic moments on the Ce ions arranged in a spin density wave with an incommensurate period (this simply means that the expectation value of the spin operator oscillates in a wavelike manner with a period that is not a rational number times a period of the crystalline lattice). This order is present at larger values of the doping x. By decreasing the value of x, or by placing the crystal under pressure, it is possible to destroy the magnetic order in a second-order quantum phase transition. The ground state then becomes a Fermi liquid with a rather large effective mass for the fermionic quasiparticles. This transition will be discussed in Chapter 12.
- The two-dimensional electron gas in semiconductor heterostructures has a very rich phase diagram with a large number of quantum phase transitions. Let us describe a particular class of transitions that will be relevant to the theoretical development in this book. As is well known, the energy spectrum of electrons moving in two dimensions in the presence of a perpendicular magnetic field splits into discrete, equally spaced energy levels (Landau levels), with each level having the same fixed macroscopic degeneracy. Consider a two-dimensional electron gas in a magnetic field at density such that the lowest Landau level is precisely filled (filling factor $\nu = 1$). The electronic spins are then fully polarized in the direction of the field, and the ground state is a fully polarized ferromagnet. Actually, this ferromagnetic order is induced more by the ferromagnetic exchange interactions between the electrons than by the Zeeman coupling to the external field. Now imagine bringing two such ferromagnetic layers close to each other [410, 401, 474, 402]. For large layer spacing, the two layers will have their ferromagnetic moments both aligned in the direction of the applied field. For smaller spacings, there turns out to be a substantial *antiferromagnetic* exchange between the two layers, so that the ground state eventually becomes a spin singlet, created by a "bonding" of electrons in opposite layers into spin singlet pairs [584, 128, 129]. The transition from a fully polarized ferromagnet to a spin singlet state actually happens through two second-order quantum phase transitions via an intermediate state with "canted" antiferromagnetic order (this shall be discussed in Section 13.4).
- The low-energy spin fluctuations of the insulator La_2CuO_4 consist of quantum fluctuations in the orientations of $S = 1/2$ spins located on the sites of a square lattice. Each spin represents the magnetic states of the d-orbitals on a Cu ion. There is an antiferromagnetic exchange coupling between the spins that prefers an antiparallel orientation for neighboring spins, and the resulting Hamiltonian is the square lattice $S = 1/2$ Heisenberg antiferromagnet (the modifier "Heisenberg" indicates that the model has the full $SU(2)$ symmetry of rotations in spin space). The ground state of this model is a "Néel" state, in which the spins are polarized in opposite orientations on the two checkerboard sublattices of the square lattice. However, theoretically, we can consider a more general model with both first- and second-neighbor antiferromagnetic exchange. As we shall discuss in Chapter 13, such a model can undergo a quantum phase transition in which the Néel order is destroyed, and the ground state becomes a quantum paramagnet with a gap to all spin excitations. While such a phase transition has not been observed experimentally so far, it still pays to consider the physics of this quantum critical point and to understand the finite-temperature crossovers in its vicinity. These crossovers also influence the behavior of the nearest

neighbor model found in La_2CuO_4, and they turn out to be a useful way of interpreting its magnetic properties at intermediate temperatures; see Chapters 5, 7, and 13.

1.4 Theoretical Models

The physics underlying the quantum transitions discussed above is quite complex and, in many cases, not completely understood. Our strategy in this book will be to thoroughly analyze the physical properties of quantum phase transitions in two simple theoretical model systems in Part II: the quantum Ising and rotor models; fortunately, these simple models also have some direct experimental applications and these will be noted at numerous points in Part II. Part III will then survey some important quantum phase transitions in other models of physical interest. Our motivation in dividing the discussion in this manner is mainly pedagogical: The quantum transitions of the Ising/rotor models have an essential simplicity, but their behavior is rich enough to display most of the basic phenomena we wish to explore. It will therefore pay to first meet the central physical ideas in this simple context.

We will introduce the quantum Ising and rotor models in turn, discussing the nature of the quantum phase transitions in them.

1.4.1 Quantum Ising Model

We begin by writing down the Hamiltonian of the quantum Ising model. It is

$$H_I = -Jg \sum_i \hat{\sigma}_i^x - J \sum_{\langle ij \rangle} \hat{\sigma}_i^z \hat{\sigma}_j^z. \tag{1.5}$$

As in the general notation introduced above, $J > 0$ is an exchange constant, which sets the microscopic energy scale, and $g > 0$ is a dimensionless coupling, which will be used to tune H_I across a quantum phase transition. The quantum degrees of freedom are represented by operators $\hat{\sigma}_i^{z,x}$, which reside on the sites, i, of a hypercubic lattice in d dimensions; the sum $\langle ij \rangle$ is over pairs of nearest neighbor sites i, j. The $\hat{\sigma}_i^{x,z}$ are the familiar Pauli matrices; the matrices on different sites i act on different spin states, and so matrices with $i \neq j$ commute with each other. In the basis where the $\hat{\sigma}_i^z$ are diagonal, these matrices have the well-known form

$$\hat{\sigma}^z = \begin{pmatrix} 1 & 0 \\ 0 & -1 \end{pmatrix}; \quad \hat{\sigma}^y = \begin{pmatrix} 0 & -i \\ i & 0 \end{pmatrix}; \quad \hat{\sigma}^x = \begin{pmatrix} 0 & 1 \\ 1 & 0 \end{pmatrix} \tag{1.6}$$

on each site i. We will denote the eigenvalues of $\hat{\sigma}_i^z$ simply by σ_i^z, and so σ_i^z takes the values ± 1. We identify the two states with eigenvalues $\sigma_i^z = +1, -1$ as the two possible orientations of an "Ising spin," which can oriented up or down in $|\uparrow\rangle_i, |\downarrow\rangle_i$. Consequently at $g = 0$, when H_I involves only the $\hat{\sigma}_i^z$, H_I will be diagonal in the basis of eigenvalues of $\hat{\sigma}_i^z$, and it reduces simply to the familiar classical Ising model. However, the $\hat{\sigma}_i^x$ are off-diagonal in the basis of these states, and therefore they induce quantum-mechanical tunneling events that flip the orientation of the Ising spin on a site. The physical significance of the two terms in H_I should be clear in the context of our earlier discussion in Section 1.3 for $LiHoF_4$. The term proportional to J is the magnetic interaction between the spins, which prefers their global ferromagnetic alignment; the actual interaction in $LiHoF_4$ has a long-range dipolar nature, but we have simplified this here to a nearest neighbor interaction. The term

proportional to Jg is the external transverse magnetic field, which disrupts the magnetic order.

Let us make these qualitative considerations somewhat more precise. The ground state of H_I can depend only upon the value of the dimensionless coupling g, and so it pays to consider the two opposing limits $g \gg 1$ and $g \ll 1$.

First consider $g \gg 1$. In this case the first term in (1.5) dominates, and, to leading order in $1/g$, the ground state is simply

$$|0\rangle = \prod_i |\rightarrow\rangle_i, \tag{1.7}$$

where

$$\begin{aligned} |\rightarrow\rangle_i &= (|\uparrow\rangle_i + |\downarrow\rangle_i)/\sqrt{2}, \\ |\leftarrow\rangle_i &= (|\uparrow\rangle_i - |\downarrow\rangle_i)/\sqrt{2} \end{aligned} \tag{1.8}$$

are the two eigenstates of $\hat{\sigma}_i^x$ with eigenvalues ± 1. The values of σ_i^z on different sites are totally uncorrelated in the state (1.7), and so $\langle 0|\hat{\sigma}_i^z \hat{\sigma}_j^z|0\rangle = \delta_{ij}$. Perturbative corrections in $1/g$ will build in correlations in σ^z that increase in range at each order in $1/g$; for g large enough these correlations are expected to remain short-ranged, and we expect in general that

$$\left\langle 0\middle|\hat{\sigma}_i^z \hat{\sigma}_j^z\middle|0\right\rangle \sim e^{-|x_i - x_j|/\xi} \tag{1.9}$$

for large $|x_i - x_j|$, where x_i is the spatial coordinate of site i, $|0\rangle$ is the exact ground state for large g, and ξ is the "correlation length" introduced above (1.2).

Next we consider the opposing limit $g \ll 1$. We will find that the nature of the ground state is qualitatively different from the large-g limit above, and we shall use this to argue that there must be a quantum phase transition between the two limiting cases at a critical $g = g_c$ of order unity. For $g \ll 1$, the second term in (1.5) coupling neighboring sites dominates; at $g = 0$ the spins are either all up or all down (in eigenstates of σ^z):

$$|\uparrow\rangle = \prod_i |\uparrow\rangle_i \quad \text{or} \quad |\downarrow\rangle = \prod_i |\downarrow\rangle_i \,. \tag{1.10}$$

Turning on a small g will mix in a small fraction of spins of the opposite orientation, but in an infinite system the degeneracy will survive at any finite order in a perturbation theory in g. This is because there is an exact global Z_2 symmetry transformation (generated by the unitary operator $\prod_i \sigma_i^x$), which maps the two ground states into each other, under which H_I remains invariant:

$$\hat{\sigma}_i^z \rightarrow -\hat{\sigma}_i^z, \qquad \hat{\sigma}_i^x \rightarrow \hat{\sigma}_i^x, \tag{1.11}$$

and there is no tunneling matrix element between the majority up and down spin sectors of the infinite system at any finite order in g. The mathematically alert reader will note that establishing the degeneracy to all orders in g, is not the same thing as establishing its existence for any small nonzero g, but more sophisticated considerations show that this is indeed the case. A thermodynamic system will always choose one or the other of the states as its ground states (which may be preferred by some infinitesimal external perturbation), and this is commonly referred to as a "spontaneous breaking" of the Z_2 symmetry. As in the large-g limit, we can characterize the ground states by the behavior of correlations of

$\hat{\sigma}_i^z$; the nature of the states (1.10) and the small-g perturbation theory suggest that

$$\lim_{|x_i - x_j| \to \infty} \langle 0 | \hat{\sigma}_i^z \hat{\sigma}_j^z | 0 \rangle = N_0^2, \tag{1.12}$$

where $|0\rangle$ is either of the ground states obtained from $|\uparrow\rangle$ or $|\downarrow\rangle$ by perturbation theory in g, and $N_0 \neq 0$ is the "spontaneous magnetization" of the ground state. This identification is made clearer by the simpler statement

$$\langle 0 | \hat{\sigma}_i^z | 0 \rangle = \pm N_0, \tag{1.13}$$

which also follows from the perturbation theory in g. We have $N_0 = 1$ for $g = 0$, but quantum fluctuations at small g reduce N_0 to a smaller, but nonzero, value.

Now we make the simple observation that it is not possible for states that obey (1.9) and (1.12) to transform into each other analytically as a function of g. There must be a critical value $g = g_c$ at which the large $|x_i - x_j|$ limit of the two-point correlator changes from (1.9) to (1.12) – this is the position of the quantum phase transition, which shall be the focus of intensive study in this book. Our arguments so far do not exclude the possibility that there could be more than one critical point, but this is known not to happen for H_I, and we will assume here that there is only one critical point at $g = g_c$. For $g > g_c$ the ground state is, as noted earlier, a *quantum paramagnet*, and (1.9) is obeyed. We will find that as g approaches g_c from above, the correlation length, ξ, diverges as in (1.2). Precisely at $g = g_c$, neither (1.9) nor (1.12) is obeyed, and we find instead a power-law dependence on $|x_i - x_j|$ at large distances. The result (1.12) holds for all $g < g_c$, when the ground state is *magnetically ordered.* The spontaneous magnetization of the ground state, N_0, vanishes as a power law as g approaches g_c from below.

Finally, we make a comment about the excited states of H_I. In a finite lattice, there is necessarily a nonzero energy separating the ground state and the first excited state. However, this energy spacing can either remain finite or approach zero in the infinite lattice limit, the two cases being identified as having a gapped or gapless energy spectrum respectively. We will find that there is an energy gap Δ that is nonzero for all $g \neq g_c$, but that it vanishes upon approaching g_c as in (1.1), producing a gapless spectrum at $g = g_c$.

1.4.2 Quantum Rotor Model

We turn to the somewhat less familiar quantum rotor models. Elementary quantum rotors do not exist in nature; rather, each quantum rotor is an effective quantum degree of freedom for the low energy states of a small number of closely coupled electrons. We will first define the quantum mechanics of a single rotor and then briefly motivate how it might represent some physically interesting systems. More details on this physical mapping will appear in Section 5.1.1.1 and Chapters 10, 13.

Each rotor can be visualized as a particle constrained to move on the surface of a (fictitious) $(N > 1)$-dimensional sphere. The orientation of each rotor is represented by an N-component unit vector $\hat{\mathbf{n}}_i$ which satisfies

$$\hat{\mathbf{n}}^2 = 1. \tag{1.14}$$

The caret on $\hat{\mathbf{n}}_i$ reminds us that the orientation of the rotor is a quantum mechanical operator, while i represents the site on which the rotor resides; we will shortly consider an infinite number of such rotors residing on the sites of a d-dimensional lattice. Each rotor has a

momentum $\hat{\mathbf{p}}_i$, and the constraint (1.14) implies that this must be tangent to the surface of the N-dimensional sphere. The rotor position and momentum satisfy the usual commutation relations

$$[\hat{n}_\alpha, \hat{p}_\beta] = i\delta_{\alpha\beta} \tag{1.15}$$

on each site i; here $\alpha, \beta = 1 \ldots N$. (Here, and in the remainder of the book, we will always measure time in units in which

$$\hbar = 1, \tag{1.16}$$

unless stated explicitly otherwise. This is also a good point to note that we will also set Boltzmann's constant

$$k_B = 1 \tag{1.17}$$

by absorbing it into the units of temperature, T.) We will actually find it more convenient to work with the $N(N-1)/2$ components of the rotor angular momentum

$$\hat{L}_{\alpha\beta} = \hat{n}_\alpha \hat{p}_\beta - \hat{n}_\beta \hat{p}_\alpha. \tag{1.18}$$

These operators are the generators of the group of rotation in N dimensions, denoted $\mathrm{O}(N)$. Their commutation relations follow straightforwardly from (1.15) and (1.18). The case $N = 3$ will be of particular interest to us: For this we define $\hat{L}_\alpha = (1/2)\epsilon_{\alpha\beta\gamma} L_{\beta\gamma}$ (where $\epsilon_{\alpha\beta\gamma}$ is a totally antisymmetric tensor with $\epsilon_{123} = 1$), and then the commutation relation between the operators on each site are

$$\begin{aligned} [\hat{L}_\alpha, \hat{L}_\beta] &= i\epsilon_{\alpha\beta\gamma}\hat{L}_\gamma, \\ [\hat{L}_\alpha, \hat{n}_\beta] &= i\epsilon_{\alpha\beta\gamma}\hat{n}_\gamma, \\ [\hat{n}_\alpha, \hat{n}_\beta] &= 0; \end{aligned} \tag{1.19}$$

the operators with different site labels all commute.

The dynamics of each rotor is governed simply by its kinetic energy term; interesting effects will arise from potential energy terms that couple the rotors together, and these will be considered momentarily. Each rotor has the kinetic energy

$$H_K = \frac{J\tilde{g}}{2}\,\hat{\mathbf{L}}^2, \tag{1.20}$$

where $1/J\tilde{g}$ is the rotor moment of inertia (we have put a tilde over g as we wish to reserve g for a different coupling to be introduced below). The Hamiltonian H_K can be readily diagonalized for general values of N by well-known group theoretical methods. We quote the results for the physically important cases of $N = 2$ and 3. For $N = 2$ the eigenvalues are

$$J\tilde{g}\ell^2/2 \quad \ell = 0, 1, 2, \ldots; \quad \text{degeneracy} = 2 - \delta_{\ell,0}. \tag{1.21}$$

Note that there is a nondegenerate ground state with $\ell = 0$, while all excited states are two-fold degenerate, corresponding to a left- or right-moving rotor. In physical applications, these states can be visualized as the low-lying energy levels of a superconducting quantum dot: ℓ measures the deviation in the number of Cooper pairs on the dot from the number found in the ground state, and $J\tilde{g}$ is a measure of the inverse self-capacitance of the dot.

More details on this physical application of $N = 2$ quantum rotors will appear in Chapter 10. For $N = 3$, the eigenvalues of H_K are

$$J\tilde{g}\ell(\ell+1)/2 \quad \ell = 0, 1, 2, \ldots; \quad \text{degeneracy} = 2\ell + 1, \tag{1.22}$$

corresponding to the familiar angular momentum states in three dimensions. These states can be viewed as representing the eigenstates of an even number of antiferromagnetically coupled Heisenberg spins. The ground state is a spin singlet, as can be expected from an antiferromagnetic coupling that prefers spins in opposite orientations. This mapping will be discussed more explicitly in Section 5.1.1.1 and in Chapter 13, where will see that there is a general and powerful correspondence between quantum antiferromagnets and $N = 3$ rotors. The O(3) quantum rotors also describe the double layer quantum Hall systems discussed in Section 1.3 [128, 129].

We are ready to write down the full quantum rotor Hamiltonian, which shall be the focus of intensive study in Part II. It is

$$H_R = \frac{J\tilde{g}}{2} \sum_i \hat{\mathbf{L}}_i^2 - J \sum_{\langle ij \rangle} \hat{\mathbf{n}}_i \cdot \hat{\mathbf{n}}_j. \tag{1.23}$$

We have augmented the sum of kinetic energies of each site with a coupling, J, between rotor orientations on neighboring sites. This coupling energy is minimized by the simple "magnetically ordered" state in which all the rotors are oriented in the same direction. In contrast, the rotor kinetic energy is minimized when the orientation of the rotor is maximally uncertain (by the uncertainty principle), and so the first term in H_R prefers a quantum paramagnetic state in which the rotors do not have a definite orientation (i.e., $\langle \mathbf{n} \rangle = 0$). Thus the roles of the two terms in H_R closely parallel those of the terms in the Ising model H_I. As in Section 1.4.1, for $\tilde{g} \gg 1$, when the kinetic energy dominates, we expect a quantum paramagnet in which, following (1.9),

$$\langle 0 | \hat{\mathbf{n}}_i \cdot \hat{\mathbf{n}}_j | 0 \rangle \sim e^{-|x_i - x_j|/\xi}. \tag{1.24}$$

Similarly, for $\tilde{g} \ll 1$, when the coupling term dominates, we expect a magnetically ordered state in which, as in (1.12),

$$\lim_{|x_i - x_j| \to \infty} \langle 0 | \hat{\mathbf{n}}_i \cdot \hat{\mathbf{n}}_j | 0 \rangle = N_0^2. \tag{1.25}$$

Finally, we can anticipate a second-order quantum phase transition between the two phases at $\tilde{g} = \tilde{g}_c$, and the behavior of N_0 and ξ upon approaching this point will be similar to that in the Ising case. These expectations turn out to be correct for $d > 1$, but we will see that they need some modifications for $d = 1$. In one dimension, we will show that $\tilde{g}_c = 0$ for $N \geq 3$, and so the ground state is a quantum paramagnetic state for all nonzero $\tilde{g}$. The case $N = 2$, $d = 1$ is special: There is a transition at a finite $\tilde{g}_c$, but the divergence of the correlation length does not obey (1.2) and the long-distance behavior of the correlation function $\tilde{g} < \tilde{g}_c$ differs from (1.25). This case will not be considered until Section 14.3 in Part III.